Received: 22 February 2022 | Revised: 12 April 2022 | Accepted: 25 April 2022 | Published online: 5 June 2022

DOI: 10.1002/trc2.12306

Alzheimer's & Dementia
Translational Research & Clinical Interventions

RESEARCH ARTICLE

In silico exploration of amyloid-related imaging abnormalities in the gantenerumab open-label extension trials using a semi-mechanistic model

Roxana Aldea[1] | **Hans Peter Grimm**[1] | **Ronald Gieschke**[1] | **Carsten Hofmann**[1] | **Dominik Lott**[1] | **Szofia Bullain**[2] | **Paul Delmar**[2] | **Gregory Klein**[1] | **Marco Lyons**[3] | **Fabrizio Piazza**[4] | **Roxana O. Carare**[5] | **Norman A. Mazer**[1]

[1]Roche Pharma Research and Early Development, Roche Innovation Center, Basel, Switzerland

[2]Roche Product Development, Neuroscience, Basel, Switzerland

[3]Roche Products Ltd, Welwyn Garden City, UK

[4]School of Medicine, Laboratory of CAA and AD Translational Research and Biomarkers, University of Milano-Bicocca, Monza, Italy

[5]Faculty of Medicine, Interdisciplinary Dementia and Aging Centre, University of Southampton, Southampton, UK

Correspondence
Roxana Aldea, Roche Innovation Center Basel, Grenzacherstrasse 124, 4070 Basel, Switzerland.
E-mail: roxana.aldea@roche.com

Abstract

Introduction: Amyloid-related imaging abnormalities with edema/effusion (ARIA-E) are commonly observed with anti-amyloid therapies in Alzheimer's disease. We developed a semi-mechanistic, in silico model to understand the time course of ARIA-E and its dose dependency.

Methods: Dynamic and statistical analyses of data from 112 individuals that experienced ARIA-E in the open-label extension of SCarlet RoAD (a study of gantenerumab in participants with prodromal Alzheimer's disease) and Marguerite RoAD (as study of Gantenerumab in participants with mild Alzheimer's disease) studies were used for model building. Gantenerumab pharmacokinetics, local amyloid removal, disturbance and repair of the vascular wall, and ARIA-E magnitude were represented in the novel vascular wall disturbance (VWD) model of ARIA-E.

Results: The modeled individual-level profiles provided a good representation of the observed pharmacokinetics and time course of ARIA-E magnitude. ARIA-E dynamics were shown to depend on the interplay between drug-mediated amyloid removal and intrinsic vascular repair processes.

Discussion: Upon further refinement and validation, the VWD model could inform strategies for dosing and ARIA monitoring in individuals with an ARIA-E history.

KEYWORDS
Alzheimer's disease, amyloid beta, amyloid-related imaging abnormalities, gantenerumab, in silico, modeling, pathophysiology, semi-mechanistic, vascular wall disturbance

1 | BACKGROUND

Over the last decades, amyloid beta (Aβ) aggregates have been the most common target of clinical trials investigating disease-modifying therapies in Alzheimer's disease (AD).[1,2] Several therapies based on monoclonal antibodies against Aβ aggregates reported amyloid-related imaging abnormalities (ARIA) within the 10% to 42% range.[3–10] Spontaneous ARIA events have been seen in the placebo arm (e.g., <3% ARIA with edema/effusion [ARIA-E] incidence) and outside the setting of anti-amyloid clinical trials.[6,7,10–13] An example of the latter are the spontaneous ARIA events occurring in cerebral amyloid angiopathy-related inflammation, a rare autoimmune encephalopathy associated with increased cerebrospinal fluid levels of anti-Aβ autoantibodies.[12,13]

Two ARIA types have been identified by magnetic resonance imaging (MRI) of the brain.[14] ARIA-E, manifested as hyperintensities on T_2-weighted fluid attenuated inversion recovery (FLAIR) images, are suggestive of vasogenic edema and sulcal effusion. ARIA-H, manifested as hypointensities on T_2*-weighted gradient echo sequences, are thought to represent hemosiderosis and microhemorrhages.[14] ARIA-E is transient and typically resolves within months, whereas ARIA-H remains visible on subsequent MRI.[3,7,10,15] As assessed with various radiological scales that show good correlation, most ARIA-E events are mild to moderate in severity and are usually not associated with symptoms.[6,7,10,16–19]

The risk of therapy-related ARIA appears to be dose-dependent and increases in apolipoprotein E (*APOE*) ε4 carriers, but the exact pathophysiological mechanisms of ARIA remain to be elucidated.[3,10,14,20] It has been proposed that the drug-mediated removal of Aβ aggregates can increase the permeability of the cerebrovascular wall to the entrance of fluid and blood products into the brain, leading to ARIA-E and ARIA-H, respectively.[14] In the AD brain, the Aβ aggregates are found in the brain parenchyma, as well as in the wall of cerebral blood vessels in the form of cerebral amyloid angiopathy (CAA).[21] Some of the anti-amyloid antibodies associated with ARIA can bind multiple forms of Aβ aggregates, such as oligomers, protofibril, fibrils, and plaques,[8] while others are directed only toward the amyloid plaques.[7] The amyloid aggregates are then degraded and/or removed through effector cell-mediated phagocytosis.[5,7,11,15] The main pathophysiological pathways thought to connect the drug-mediated removal of Aβ aggregates to ARIA are depicted in Figure 1.[3,8,15,21–26] All postulated ARIA pathomechanisms appear to include some degree of disturbance in the cerebrovascular wall. It remains unclear to what extent the degree of amyloid burden, or the location and rate of amyloid clearance, influence the onset, time course, and severity of ARIA.[21,27] Gaining a better understanding of ARIA etiology has the potential to unveil additional risk factors that could accelerate the path toward patient-centric safety strategies for anti-amyloid therapies.

The aim of the current work is to explain the temporal dynamics and dose-dependency of ARIA-E severity by developing a semi-mechanistic, in silico model of ARIA-E, referred to as the VWD model. The mathematical framework of the VWD model allows different biological interpretations of the modeled mechanisms, in line with the ARIA-E pathomechanisms proposed in Figure 1. It is hypothesized that the interplay between drug-mediated removal of local amyloid and intrinsic vascular repair processes determines the level of VWD, which further influences the magnitude of ARIA-E.

RESEARCH IN CONTEXT

1. **Systematic Review**: The authors reviewed published literature and conference materials. Several publications discuss potential pathophysiological mechanisms of amyloid-related imaging abnormalities (ARIA). However, a computational framework that explores the postulated mechanisms of ARIA in the context of longitudinal, patient-level observations of ARIA from anti-amyloid trials is missing.
2. **Interpretation**: We developed the first in silico model that proposes a parsimonious mathematical representation of multiple hypotheses thought to underlie ARIA-edema/effusion (ARIA-E). The novel vascular wall disturbance (VWD) model of ARIA-E provides a good description of the temporal dynamics and dose-dependency of ARIA-E severity observed in two gantenerumab studies, thereby confirming the plausibility of the modeled mechanisms.
3. **Future Directions**: The predictive power of the VWD model remains to be tested with forthcoming ARIA data from ongoing anti-amyloid clinical trials. Upon validation, this model could support decisions on re-dosing and safety monitoring of individuals that experienced ARIA-E with anti-amyloid treatment.

2 | METHODS

2.1 | Clinical studies and ARIA assessment

The SCarlet RoAD (SR); (A Study of Gantenerumab in Participants with Prodromal Alzheimer's Disease, NCT01224106) and Marguerite RoAD (MR); (A Study of Gantenerumab in Participants with Mild Alzheimer's Disease, NCT02051608) studies of gantenerumab included participants with prodromal AD and mild AD, respectively, as previously described.[6,28] The SR/MR study participants who received the double-blind treatment and had at least one follow-up visit were eligible for open label extension (OLE) study participation. During the SR/MR OLE studies, all participants received subcutaneous gantenerumab every 4 weeks, with gradual up-titration toward the target dose of 1200 mg. Each participant was assigned to one of five dose titration regimens based on their *APOE* ε4 carrier status and the last dose during the double-blind treatment (Table S1 in supporting information). Protocol-defined routine magnetic resonance imaging (MRI)

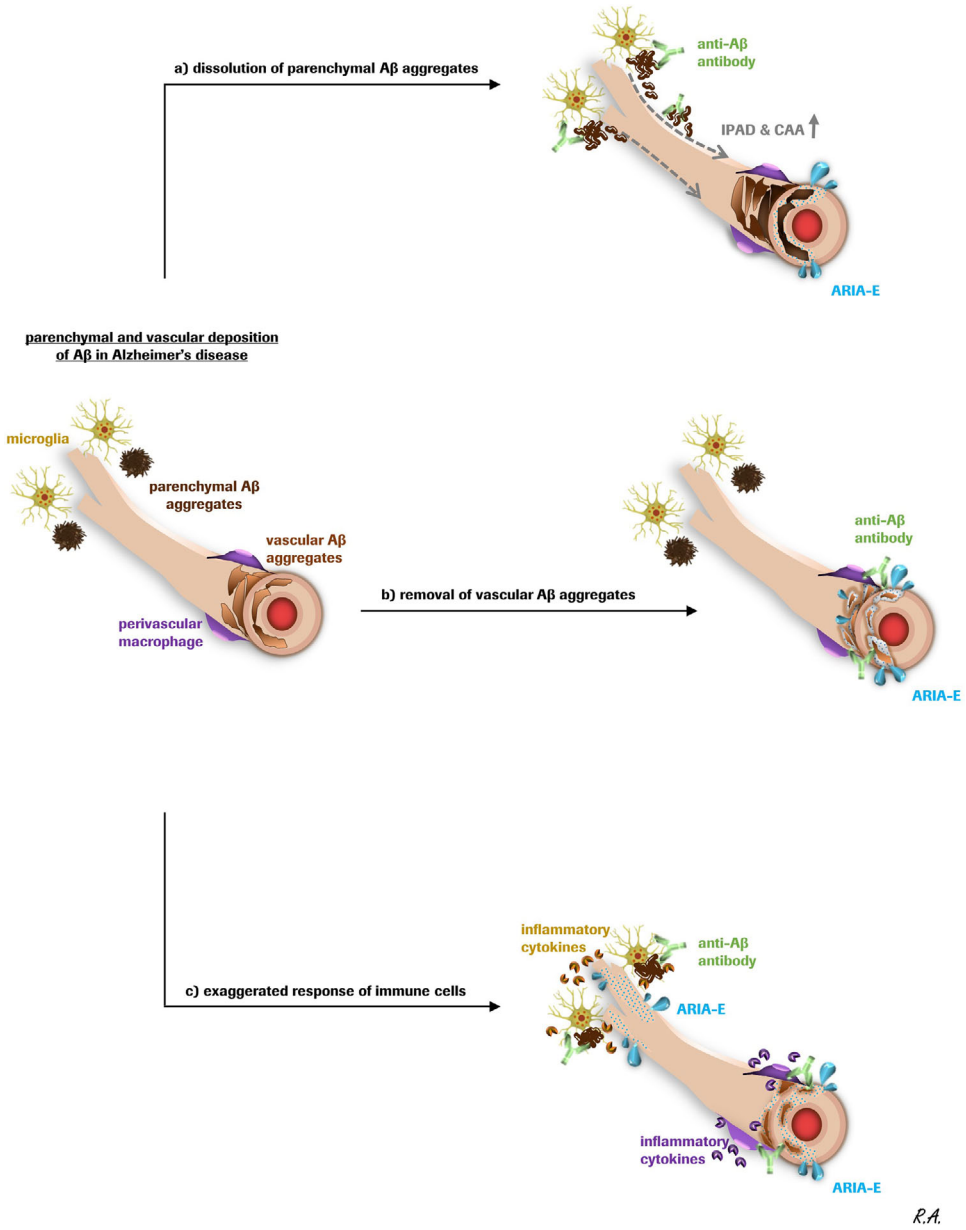

FIGURE 1 Mechanistic pathways underlying the amyloid-related imaging abnormalities with edema/effusion (ARIA-E) associated with anti-amyloid beta (Aβ) therapies. In Alzheimer's disease, Aβ proteins aggregate in brain parenchyma, as well as in the cerebrovascular wall as cerebral amyloid angiopathy (CAA). All the pathophysiological mechanisms thought to drive therapy-induced ARIA include some degree of disturbance in the cerebrovascular wall. A, Drug-induced dissolution of parenchymal Aβ aggregates with subsequent movement of Aβ into the vessel wall poses a higher burden on the intramural periarterial drainage (IPAD) pathways, accelerating the vascular deposition of Aβ and aggravating the CAA-related vascular damage. B, Drug-induced removal of vascular Aβ aggregates disrupts the integrity of the cerebrovascular wall, promoting leakage of fluid into the brain. C, Drug-mediated phagocytosis of Aβ aggregates induces an exaggerated inflammatory response of vessel-associated immune cells, such as microglia and perivascular macrophages, thereby locally perturbing the permeability of adjacent vessels to fluid entrance into the brain. In addition to fluid entrance, blood products may also leak through the vessel wall into the tissue, leading to ARIA-H. Depending on the drug's mode of action, these mechanisms could co-occur; however, for visibility reasons, they are illustrated separately. The novel mathematical model of ARIA-E, called the vascular wall disturbance (VWD) model, can be biologically interpreted from the perspective of all the aforementioned mechanisms. Schematic drawing by Roxana Aldea

monitoring for ARIA detection was performed at regular intervals. If ARIA was detected, dosing was adjusted based on its radiological severity and/or presence of symptoms, as described in supporting information. The magnitude of ARIA-E on MRI scans was assessed with the Barkhof Grand Total Scale (BGTS), a 60-point severity scale on which higher scores indicate greater severity.[16,17] The work described was carried out in accordance with the Declaration of Helsinki and study participants provided written informed consent.

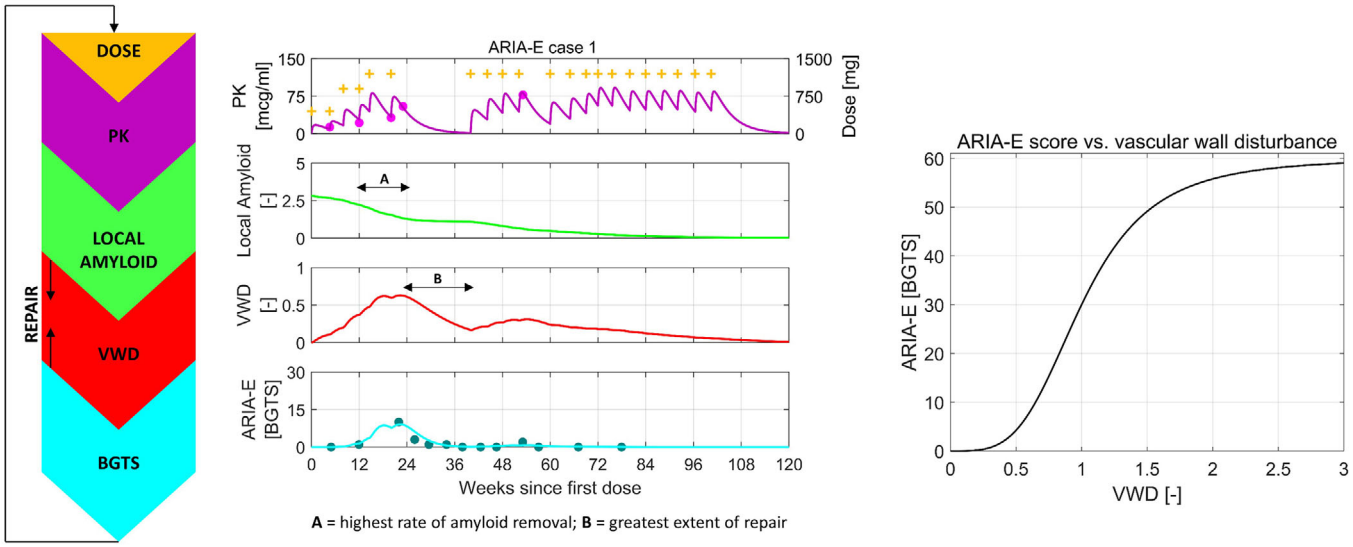

FIGURE 2 The key modules of the vascular wall disturbance (VWD) model of amyloid-related imaging abnormalities with edema/effusion (ARIA-E) and the behavior of the model at the individual level. The VWD model links several pharmacological and biological factors to the observed drug pharmacokinetics and magnitude of ARIA-E (purple and cyan filled circles, respectively). Individual-specific information about the dose and time of drug administration is given (yellow symbols). The "PK" module, that is, pharmacokinetics, describes the time course of drug concentration "Local Amyloid" module estimates the drug-mediated change in local amyloid over time (green curve) under the assumption that the rate of amyloid removal is proportional to both existing local amyloid level and drug concentration in plasma. The instantaneous rate of drug-mediated amyloid removal corresponds to the steepness of the amyloid curve at any given time point. The modeled amyloid is not the positron emission tomography amyloid measured in the clinical trial, but rather a hypothetical measure for either the local vascular amyloid or the local parenchymal amyloid load, whose removal may trigger a cascade of events resulting in ARIA-E in one or more regions of the brain. The "VWD" module estimates temporal changes in the "vascular wall disturbance" variable (red curve), which is a hypothetical measure of susceptibility to fluid leakage into the brain due to disrupted vascular integrity and/or perivascular inflammation. The increase in vascular wall disturbance is driven by drug-mediated amyloid removal and counteracted by an intrinsic repair process of the vascular wall. The "BGTS" (Barkhof's Grand Total Scale) module relates the vascular wall disturbance level to the ARIA-E score (BGTS) in a non-linear (sigmoidal) fashion, as shown in the right-hand side graph. The sigmoidal relationship was derived from the overall data and assumed to be the same for each patient. Individual dosing can be adjusted based on the value of BGTS. The observed BGTS is given by the cyan filled circles and the model fit by the cyan curve

2.2 | Participant data used in modeling

Longitudinal measurements of drug concentration in plasma and of ARIA-E magnitude from 112 individuals who developed ARIA-E during the OLE SR/MR phase III trials were used for model building. The individuals included in the model are all the study participants that experienced their first ARIA-E, that is, had a FLAIR scan with BGTS > 0, within 1 year after the first dose of gantenerumab in the OLE period, as of May 29, 2018. During their double-blind period, the study participants included in this model were on relatively low doses and most of their MRI scans showed no ARIA-E. For this reason, the double-blind period was not used for model development.

2.3 | In silico implementation of the ARIA-E VWD model

The ARIA-E VWD model was developed as a semi-mechanistic pharmacokinetic-pharmacodynamic (PKPD) model that integrates known and presumed biological processes and accounts for inter-individual variability of model parameters. The key modules of the ARIA-E VWD model are depicted in Figure 2 and the mathematical representation is given in supporting information. A previously developed population PK model[29] was used to generate individual concentration-time profiles for the ARIA-E cases of interest considering each patient's individual dosing history and longitudinal observations of drug concentration in plasma. The PD model is novel and comprises a mixture of ordinary differential and algebraic equations. All model parameters were estimated using a nonlinear mixed effects modeling approach.[30] Hereinafter, the focus is on individual-based model predictions. Model evaluation and selection was based on multiple criteria, including robust estimation of parameters and good agreement between model predictions and observations (see supporting information). Upon model fitting to longitudinal BGTS observations, the influence of key model parameters on ARIA-E evolution was explored with individual-level simulations explained in supporting information.

3 | RESULTS

3.1 | Mechanistic aspects of the ARIA-E VWD model

The proposed VWD model shown in Figure 2 interconnects the following factors: (1) gantenerumab doses; (2) drug concentration in plasma; (3) drug-induced removal of local amyloid, which

represents a hypothetical measure of either the vascular or the parenchymal amyloid from the brain regions affected by ARIA-E;[21] (4) the build-up of VWD, a hypothetical concept that describes the susceptibility to fluid leakage into the brain due to therapy-induced defects in the vascular and perivascular structures of the brain, such as impaired blood-brain barrier and burdened intramural periarterial drainage pathways;[3,31] (5) an intrinsic vascular repair process presumed to counteract the VWD build-up; and (6) the BGTS that quantifies the severity of ARIA-E. Individual-specific information about the given dose and time of administration is known, while the parameters related to all the other factors are estimated.

The local amyloid is removed at a rate assumed proportional to both drug concentration in plasma and existing local amyloid level. The proportionality factor, here denoted $\alpha_{removal}$ and referred to as the removal constant, could be interpreted as the rate constant of the biochemical reaction between anti-amyloid antibodies and amyloid aggregates. Such a reaction is required for the drug-mediated amyloid removal to occur and its magnitude may vary across individuals. For anti-amyloid antibodies that rely heavily on Fc receptor-mediated phagocytosis of amyloid aggregates by immune cells, the removal constant could reflect the response of the immune cells, such as microglia and perivascular macrophages, activated by the amyloid-drug complex. The baseline level of local amyloid (here denoted $Amyloid_0$) impacts the initial rate of amyloid removal and may also vary across individuals. Other processes that could alter the amyloid level, such as amyloid production and endogenous amyloid clearance, are not included in the model.

Drug-mediated amyloid removal is assumed to drive the VWD buildup, which is counteracted by a presumed intrinsic vascular repair process. The vascular repair is assumed to be a first-order process with a rate constant (k_{repair}). The VWD magnitude is related to BGTS according to the sigmoidal function illustrated in Figure 2. This relationship ensures small BGTS at low VWD levels, a sharp rise in BGTS at intermediate VWD levels, and imposes an upper limit for ARIA-E magnitude (BGTS = 60) at high VWD levels.

The mathematical representation of the aforementioned relationships is given in supporting information. The estimated values of all model parameters are reported in Table S2 in supporting information. The parameters $Amyloid_0$, $\alpha_{removal}$, and k_{repair} are allowed to vary across patients, following the statistical distribution shown in Figure 3 and discussed in Section 3.2.

The modeled drug concentrations compare well with the observed ones, as shown in Figures 2, 3, and S1 in supporting information. The predicted levels of local amyloid cannot be verified in this work considering that imaging of local amyloid was unavailable. The model predictions for the disturbance and repair of the vascular wall also await verification contingent on additional/novel biomarkers capable of quantifying focal and transient damages of the cerebrovascular wall. Finally, the modeled BGTS values generally compare well with the observed ones, as shown in Figures 2, 3, and S2 in supporting information.

3.2 | Dynamical behavior of illustrative cases

To illustrate the properties of the VWD model, we discuss four ARIA-E cases summarized in Table S3 in supporting information. These cases are chosen to highlight a variety of ARIA-E features (magnitude, resolution, recurrence) that are mechanistically insightful, but do not reflect the typical ARIA-E profile of gantenerumab. Each study participant was assigned to 1 to 5 dose titration regimens described in Table S1. Because the model accounted for inter-individual variability, the modeled temporal profiles of each ARIA-E case are generated based on empirical Bayes estimates, that is, the most probable values of the individual parameters.

Cases 1 and 2 were assigned to the same fast up-titration regimen (regimen 4) but, nonetheless, developed ARIA-E at significantly different times (Figures 2 and 3). Case 1 reached the target dose by week 16 and experienced the first ARIA-E event that required treatment interruption at week 20, whereas case 2 developed ARIA-E at week 12 before reaching the target dose. The two cases appear to experience different rates of amyloid removal around week 12, as can be seen from the different slopes of the amyloid curves. This is explained in the model by the different estimates of the removal constant (see $\alpha_{removal}$ values in Figure 3). This difference arises despite similar drug concentration levels during the first 12 weeks and comparable estimates of baseline amyloid levels.

Case 3, assigned to the slowest up-titration regimen (regimen 1), experienced treatment interruption on two occasions due to ARIA-E (Figure 3). The development of ARIA-E during slow up-titration may be ascribed to the relatively high baseline level of local amyloid estimated for this patient (see $Amyloid_0$ values in Figure 3). The model explains the re-occurrence of ARIA-E upon re-dosing and up-titration by the combination of persisting high levels of local amyloid and relatively high drug concentrations, which drives another rise in VWD.

Case 4, assigned to the second slowest up-titration regimen (regimen 2), developed an early ARIA-E that was much higher in magnitude than any of the ARIA-E events experienced by the other three cases (Figure 3). The model does not estimate any significantly different levels of baseline local amyloid or drug concentrations that could explain the observed disparity in ARIA-E magnitude. However, both the removal and repair constants estimated for case 4 are significantly different from the constants estimated for the other three cases. Specifically, the strikingly large value of the removal constant drives amyloid removal at a high rate that cannot be matched by the slow rate of vascular repair determined by the small repair rate constant (see $\alpha_{removal}$ and k_{repair} values in Figure 3). This imbalance leads to a large VWD level and, ultimately, to a high BGTS.

The model predictions for the four ARIA-E cases share multiple features. The model predicts the steepest decrease in local amyloid and a subsequent increase in VWD and BGTS magnitude around the time of observed ARIA-E events. This pattern is noticeable at week 20 for case 1, week 12 for case 2, weeks 28 and 60 for case 3, and weeks 12 and 52 for case 4 (Figures 2 and 3). During the entire period of treatment interruption, the model predicts a plateau in the amyloid level and a

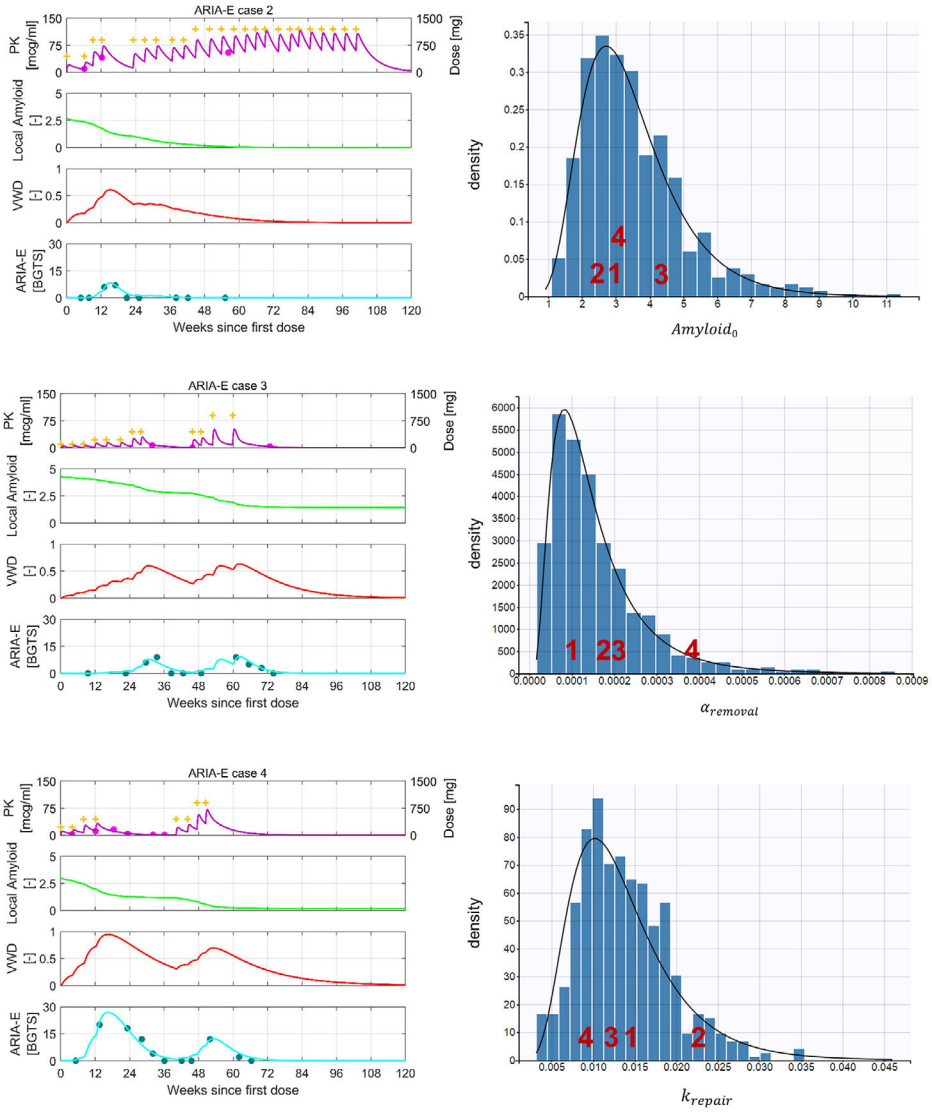

FIGURE 3 Model behavior at the patient level. The blue histograms represent the empirical distribution of the model parameters estimated with inter-individual variability, while the black curves represent the theoretical density functions. The density function of each random variable relates to its probability of falling within a particular range of values. The individual-specific parameters for the illustrated amyloid-related imaging abnormalities with edema/effusion (ARIA-E) cases are indicated as red numerals plotted at the corresponding X-value in each histogram. $Amyloid_0$ (arbitrary units) denotes the baseline level of local amyloid at the site of ARIA-E. $\alpha_{removal}$ $[(day \cdot mcg/ml)^{-1}]$ is interpreted as the removal constant that relates the rate of amyloid removal to existing local amyloid levels and drug concentration in plasma. k_{repair} (day^{-1}) denotes the first-order rate constant of the intrinsic vascular repair process. BGTS, Barkhof's Grand Total Scale; PK, pharmacokinetics; VWD, vascular wall disturbance

progressive decrease in VWD. The latter also reflects the repair process and translates into a progressive decrease in ARIA-E magnitude that closely follows the observed ARIA-E resolution, as it can be seen during weeks 20–36 for case 1, weeks 12–24 for case 2, weeks 28–44 for case 3, and weeks 12–40 for case 4 (Figures 2 and 3).

3.3 | Exploration of the influence of key model parameters in the dynamics of ARIA-E

The removal constant and the baseline level of local amyloid influence the rate of local amyloid removal; hence, their role in the dynamics of ARIA-E was explored separately in a set of simulations shown in Figure 4 in panels A and B, respectively. The larger removal constant leads to earlier increases in both VWD and ARIA-E, while the smaller one delays the ARIA-E appearance, but also slows the clearance of local amyloid; this is visible at weeks 12 and 24 in panel A. Regarding the role of baseline local amyloid, for the higher baseline level, the model predicts earlier vascular wall disturbances and recurrent ARIA-E due to persisting high levels of amyloid. In contrast, for the smaller baseline level, the model predicts continuous removal of amyloid without any significant ARIA-E (panel B).

Panel C of Figure 4 illustrates the evolution of ARIA-E when the presumed vascular repair process is reduced or intensified through the

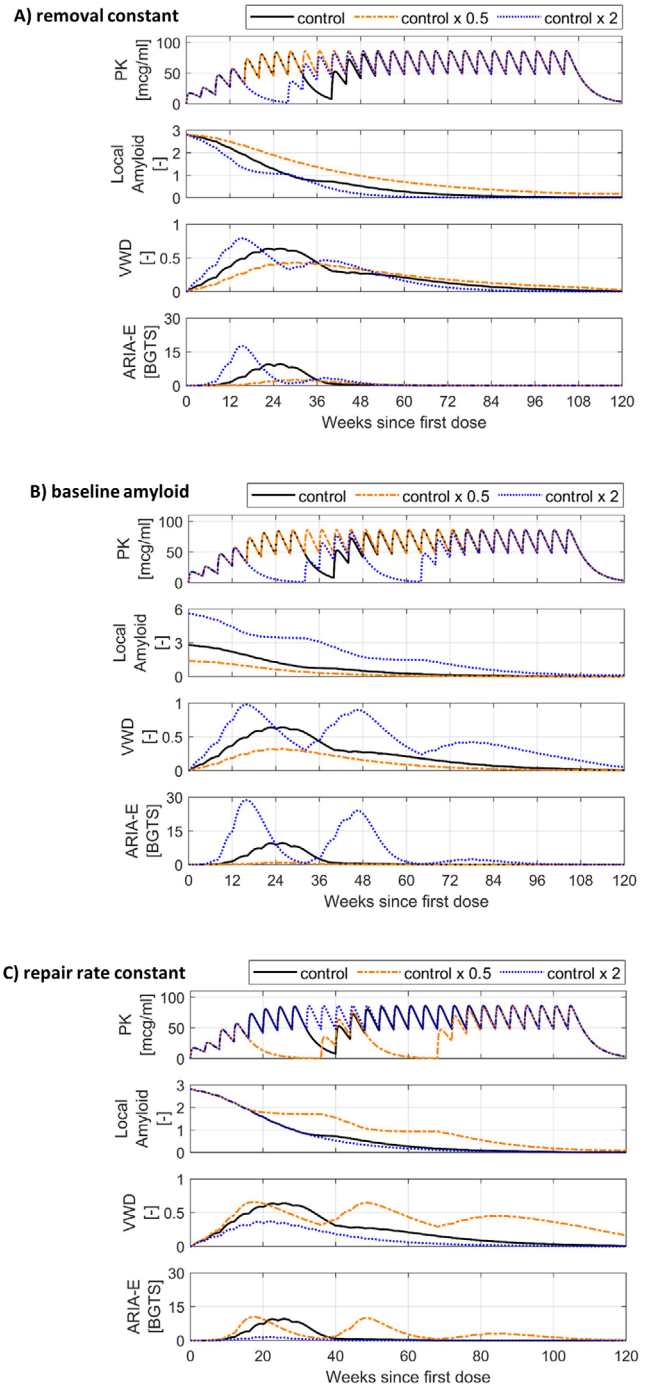

FIGURE 4 Exploring the effect of model parameters on amyloid-related imaging abnormalities with edema/effusion (ARIA-E) dynamics. In each set of simulations, only one key parameter is varied by doubling and halving the original control value, while all the other model parameters remain unchanged. The "control" temporal profiles shown in black are simulated using the model parameters estimated for ARIA-E case 1, the dosing regimen 4 shown in Table S1, and a set of simple rules for MRI monitoring and treatment interruption; these rules are created for illustrative purposes and are described in supporting information. BGTS, Barkhof's Grand Total Scale; MRI, magnetic resonance imaging; PK, pharmacokinetics; VWD, vascular wall disturbance. Simulated ARIA-E dynamics for: A) different removal constants, B) different baseline levels of local amyloid and C) different vascular repair rate constants

variation of the repair rate constant. If the intrinsic vascular repair process occurred at a smaller rate, local amyloid removal would result in repeated disturbances in the vascular wall, ultimately leading to ARIA-E recurrence. Conversely, vascular repair processes with a larger rate constant would be able to counteract the rate of amyloid removal predicted at the end of up-titration and prevent any significant ARIA-E.

4 | DISCUSSION

To the best of our knowledge, this is the first semi-mechanistic, in silico model that tackles the ambiguity and complexity of ARIA-E pathomechanisms in the context of longitudinal observations of ARIA-E magnitude from anti-amyloid clinical trials. The earlier ARIA-E models developed with bapineuzumab, gantenerumab, and aducanumab data are event hazard models that predict the probability of ARIA-E occurrence for various dosing regimens, without accounting for any specific pathomechanisms.[29,32–34] The mechanistic rationale behind the proposed VWD model complements the earlier ARIA-E hazard model that suggested dose up-titration as a way to reduce the incidence of ARIA-E events in the gantenerumab studies.[33] Here, we developed a mathematical framework that permits different biological interpretations of the modeled mechanisms, based on the following key factors: local amyloid load, drug exposure (dose and drug concentration), amyloid removal, as well as damage and repair of the vascular wall. For the various ARIA-E scenarios depicted in Figure 1, the same mathematical relationship describes the drug-mediated removal of local amyloid, whether it is the parenchymal or vascular Aβ burden that is being cleared via direct dissolution or cell-mediated phagocytosis. While the precise biological details underlying ARIA-E remain to be unveiled, the common feature across the different mechanistic pathways that can set off an ARIA-E event seems to be a damaged vascular wall. With this in mind, we formulated a set of equations that link the drug-mediated removal of local amyloid to the level of VWD and, ultimately, to the severity of ARIA-E (as measured by BGTS). The model parameters were estimated with a non-linear mixed effects method. The resulting VWD model provides a good patient-level description of the ARIA-E time-course reported in past SR/MR OLE studies of gantenerumab, thereby confirming the plausibility of the implemented mechanisms. The predictive power of the VWD model will be tested upon the completion of the ongoing GRADUATE studies that investigate an optimized 9-month titration informed by the historic OLE data.

Beyond fitting individual time courses of ARIA-E events, the VWD model offers several insights. According to the model, high rates of local amyloid removal can prompt the onset of ARIA-E due to (1) high exposure (dose and drug concentration), (2) high local amyloid, and/or (3) high efficiency in amyloid removal (here, captured by the removal constant $\alpha_{removal}$). For anti-amyloid antibodies, such as aducanumab, donanemab, and gantenerumab, which rely heavily on Fc receptor-mediated phagocytosis of amyloid aggregates by immune cells, the higher estimates of the removal constant could reflect a larger, likely exaggerated, response of the immune cells activated by the amyloid-drug complex. An image-based analysis of a small number of ARIA-E

cases from the gantenerumab studies revealed that the regions with ARIA-E often displayed prominent decreases in the amyloid positron emission tomography (PET) signal, thereby supporting the idea of more efficient cell-mediated phagocytosis of Aβ aggregates at the ARIA-E sites.[15] It is noteworthy that significant amyloid reductions were also observed in regions without any FLAIR abnormalities.[15,28,35] Based on the VWD model, one possible explanation is that focal amyloid reductions can occur without ARIA-E as long as the local rates of amyloid removal are counterbalanced by the rate of an intrinsic vascular repair process. Moreover, according to the model, ARIA-E can fully resolve (BGTS = 0) before the VWD level returns to zero. This behavior is a consequence of the presumed nonlinear VWD–BGTS relationship, which ensures that small disturbances in the vascular wall do not result in a detectable ARIA-E event, as shown in Figure 2. Last, The VWD model suggests that ARIA-E recurrent episodes could be a combined effect of high drug concentrations and persisting high levels of local amyloid and that amyloid depletion over time ultimately reduces the risk of ARIA, even at high drug concentrations. Recurrent ARIA-E events are rarely seen in anti-amyloid clinical trials;[10] nonetheless, better understanding the factors that contribute to ARIA-E recurrence will ultimately optimize the long-term management of ARIA.

When comparing the modeled reduction in local amyloid to the amyloid reductions observed in anti-amyloid clinical trials, the distinction between the global and local nature of the modeled/measured amyloid needs to be acknowledged. For instance, global PET assessments of baseline amyloid in the bapineuzumab and gantenerumab studies did not find any significant differences between the ARIA-E and non-ARIA-E groups.[35,36] When instead the amyloid PET signal was assessed regionally, the baseline amyloid load from the occipital brain region was found to be significantly higher in the ARIA-E group than in the non-ARIA-E group.[35] Accounting for the predilection of CAA for the occipital vasculature, the high baseline levels of local amyloid estimated by the VWD model could be associated with a high local burden of vascular amyloid. Based on PET imaging alone, the extent to which the reduction in amyloid PET signal is driven by the removal of vascular amyloid remains uncertain, as further discussed in supporting information.

Given that the current model seeks to provide a plausible pathophysiological explanation for the individual temporal profiles of ARIA-E seen in the gantenerumab SR/MR OLE studies, this analysis focused on the quality of the modeled individual-level profiles. To generate population predictions that support decisions on dosing and monitoring of individuals with ARIA-E, the VWD model needs to be further refined and validated. Model enrichment with biomarker data is also of paramount importance for model optimization and its translation to clinical practice. The inclusion of a broader population—especially inclusion of non-ARIA-E individuals—could offer opportunities to guide the stratification of individuals based on their risk for ARIA-E. The sparse ARIA data make this endeavor challenging, considering that a significant part of the data need to be reserved to demonstrate the predictive value of the model built on the remaining data.

In conclusion, the work presented here enhances our current understanding of ARIA-E phenomenology by providing a mathematical, semi-mechanistic explanation of the observed temporal patterns in the BGTS data of gantenerumab studies. The VWD model allows in silico individual-level exploration of biologically plausible variables and processes that influence the development and severity of ARIA-E. Upon its validation, the VWD model will be useful for the generation of hypotheses that can be tested in clinical studies for ARIA management. The VWD model could simulate the impact of the rate of local amyloid removal and vascular repair on the time course of ARIA-E in individuals with an ARIA-E history. Such model-based predictions could support decisions on the continuation or re-introduction of treatment to minimize the risk of ARIA-E progression.

ACKNOWLEDGMENTS

This work was supported by Roche. We would like to thank Sebastien Jolivet for providing data support and Martin Traber for useful discussions.

CONFLICTS OF INTEREST

RA, HPG, CH, DL, SB, PD, GK, ML, and NAM are full-time employees of F. Hoffmann-La Roche. RG is a former employee of F. Hoffmann-La Roche, currently acting as consultant for F. Hoffmann-La Roche. HPG, RG, CH, DL, SB, PD, GK, ML, and NAM are shareholders of F. Hoffmann-La Roche. FP and ROC are consultants for F. Hoffmann-La Roche. FP is the Funding Member and Coordinator of the iCAβ international Network and the CAA study Group of the Italian Society of Neurology-dementia (SINdem) and is a member of the European Alzheimer's Disease Consortium (EADC) General Assembly. He is the inventor (without ownership) of a patent for a method and kit for anti-Aβ autoantibody ultrasensitive detection of ARIA and CAA-ri. He served as a consultant and he has been involved in Global Advisory Boards on Alzheimer's disease immunotherapy and biomarkers done by Roche. He is the Principal Investigator of the ModelCAA Research Grant AARG-18-561699 funded by the Alzheimer's Association. Author disclosures are available in the supporting information.

REFERENCES

1. Anti-amyloid-β monoclonal antibodies for Alzheimer's disease: pitfalls and promise. *Biol Psychiat* 2018;83:311-319. https://doi.org/10.1016/j.biopsych.2017.08.010
2. Cummings J, Lee G, Ritter A, Sabbagh M, Zhong K. Alzheimer's disease drug development pipeline: 2020. *Alzheimer's Dement*. 2020;6:e12050. https://doi.org/10.1002/trc2.12050
3. Sperling R, Salloway S, Brooks DJ, et al. Amyloid-related imaging abnormalities in patients with Alzheimer's disease treated with bapineuzumab: a retrospective analysis. *Lancet Neurol*. 2012;11:241-249. https://doi.org/10.1016/s1474-4422(12)70015-7
4. Salloway S, Sperling R, Fox NC, et al. Two phase 3 trials of bapineuzumab in mild-to-moderate Alzheimer's disease. *N Engl J Med*. 2014;370:322-333. https://doi.org/10.1056/nejmoa1304839
5. Sevigny J, Chiao P, Bussière T, et al. The antibody aducanumab reduces Aβ plaques in Alzheimer's disease. *Nature*. 2016;537:50-56. https://doi.org/10.1038/nature19323
6. Ostrowitzki S, Lasser RA, Dorflinger E, et al. A phase III randomized trial of gantenerumab in prodromal Alzheimer's disease. Alzheimer's. *Res Ther*. 2017;9:95. https://doi.org/10.1186/s13195-017-0318-y
7. Mintun MA, Lo AC, Evans CD, et al. Donanemab in early Alzheimer's Disease. *New Engl J Med*. 2021;384:1691-1704. https://doi.org/10.1056/nejmoa2100708

8. Tolar M, Abushakra S, Hey JA, Porsteinsson A, Sabbagh M. Aducanumab, gantenerumab, BAN2401, and ALZ-801 – the first wave of amyloid-targeting drugs for Alzheimer's disease with potential for near term approval. *Alzheimer's Res Ther*. 2020;12:95. https://doi.org/10.1186/s13195-020-00663-w
9. Avgerinos KI, Ferrucci L, Kapogiannis D. Effects of monoclonal antibodies against amyloid-β on clinical and biomarker outcomes and adverse event risks: a systematic review and meta-analysis of phase III RCTs in Alzheimer's disease. *Ageing Res Rev*. 2021;68:101339. https://doi.org/10.1016/j.arr.2021.101339
10. Salloway S, Chalkias S, Barkhof F, et al. Amyloid-Related imaging abnormalities in 2 phase 3 studies evaluating aducanumab in patients with early Alzheimer disease. *JAMA Neurol*. 2022;79(1):13-21. https://doi.org/10.1001/jamaneurol.2021.4161
11. Swanson CJ, Zhang Y, Dhadda S, et al. A randomized, double-blind, phase 2b proof-of-concept clinical trial in early Alzheimer's disease with lecanemab, an anti-Aβ protofibril antibody. Alzheimer's. *Res Ther*. 2021;13:80. https://doi.org/10.1186/s13195-021-00813-8
12. Antolini L, DiFrancesco JC, Zedde M, et al. Spontaneous ARIA-like events in cerebral amyloid angiopathy – related inflammation: a multicenter prospective longitudinal cohort study. *Neurology*. 2021;97(18):e1809-e1822.
13. Piazza F, Greenberg SM, Savoiardo M, et al. Anti–amyloid β autoantibodies in cerebral amyloid angiopathy – related inflammation: implications for amyloid-modifying therapies. *Ann Neurol*. 2013;73:449-458. https://doi.org/10.1002/ana.23857
14. Sperling RA, Jack CR, Black SE, et al. Amyloid-related imaging abnormalities in amyloid-modifying therapeutic trials: recommendations from the Alzheimer's Association Research Roundtable Workgroup. Alzheimer's. *Dementia*. 2011;7:367-385. https://doi.org/10.1016/j.jalz.2011.05.2351
15. Ostrowitzki S, Deptula D, Thurfjell L, et al. Mechanism of amyloid removal in patients with Alzheimer disease treated with gantenerumab. *Arch Neurol-Chicago*. 2012;69:198-207. https://doi.org/10.1001/archneurol.2011.1538
16. Barkhof F, Daams M, Scheltens P, et al. An MRI rating scale for amyloid-related imaging abnormalities with edema or effusion. *Am J Neuroradiol*. 2013;34(8):1550-1555. https://doi.org/10.3174/ajnr.A3475
17. Bechten A, Wattjes MP, Purcell DD, et al. Validation of an MRI rating scale for amyloid-related imaging abnormalities. *J Neuroimaging*. 2017;27:318-325. https://doi.org/10.1111/jon.12422
18. Klein G, Bracoud L, Purcell DD, et al. Calibration of a simplified ARIA-E MRI severity scale suitable for clinical practice. *Alzheimer's Dement*. 2020;16(Suppl. 2):e041110. https://doi.org/10.1002/alz.041110
19. VandeVrede L, Gibbs DM, Koestler M, et al. Symptomatic amyloid-related imaging abnormalities in an APOE ε4/ε4 patient treated with aducanumab. *Alzheimer's Dement Diagnosis Assess Dis Monit*. 2020;12:e12101. https://doi.org/10.1002/dad2.12101
20. . Anti-amyloid-β monoclonal antibodies for Alzheimer's Disease: pitfalls and promise. *Biol Psychiat*. 2018;83:311-319. https://doi.org/10.1016/j.biopsych.2017.08.010
21. Greenberg SM, Bacskai BJ, Hernandez-Guillamon M, Pruzin J, Sperling R, Veluw SJV. Cerebral amyloid angiopathy and Alzheimer disease – one peptide, two pathways. *Nat Rev Neurol*. 2020;16:30-42. https://doi.org/10.1038/s41582-019-0281-2
22. Boche D, Zotova E, Weller RO, et al. Consequence of Aβ immunization on the vasculature of human Alzheimer's disease brain. *Brain*. 2008;131:3299-3310. https://doi.org/10.1093/brain/awn261
23. Cribbs DH, Berchtold NC, Perreau V, et al. Extensive innate immune gene activation accompanies brain aging, increasing vulnerability to cognitive decline and neurodegeneration: a microarray study. *J Neuroinflamm*. 2012;9:179. https://doi.org/10.1186/1742-2094-9-179
24. Zago W, Schroeter S, Guido T, et al. Vascular alterations in PDAPP mice after anti-Aβ immunotherapy: implications for amyloid-related imaging abnormalities. *Alzheimer's. Dementia*. 2013;9:S105-15. https://doi.org/10.1016/j.jalz.2012.11.010
25. Fuller JP, Stavenhagen JB, Teeling JL. New roles for Fc receptors in neurodegeneration-the impact on immunotherapy for Alzheimer's disease. *Front Neurosci-Switz*. 2014;8:235. https://doi.org/10.3389/fnins.2014.00235
26. Carare RO, Aldea R, Agarwal N, et al. Clearance of interstitial fluid (ISF) and CSF (CLIC) group – part of Vascular Professional Interest Area (PIA). *Alzheimer's Dement (Amst)*. 2020;12(1):e12053. https://doi.org/10.1002/dad2.12053
27. Piazza F, Winblad B. Amyloid-related imaging abnormalities (ARIA) in immunotherapy trials for Alzheimer's Disease: need for prognostic biomarkers? *J Alzheimer's Dis*. 2016;52:417-420. https://doi.org/10.3233/jad-160122
28. Klein G, Delmar P, Voyle N, et al. Gantenerumab reduces amyloid-β plaques in patients with prodromal to moderate Alzheimer's disease: a PET substudy interim analysis. Alzheimer's. *Res Ther*. 2019;11:101. https://doi.org/10.1186/s13195-019-0559-z
29. Retout S, Gieschke R, Serafin D, Weber C, Frey N, Hofmann C. Disease modeling and model-based meta-analyses to define a new direction for a phase iii program of gantenerumab in alzheimer's disease. *Clin Pharmacol Ther*. 2022;111(4):857-866. https://doi.org/10.1002/cpt.2535
30. Mould DR, Upton RN. Basic concepts in population modeling, simulation, and model-based drug development. *Cpt Pharmacometrics Syst Pharmacol*. 2012;1:e6. https://doi.org/10.1038/psp.2012.4
31. Weller RO, Preston SD, Subash M, Carare RO. Cerebral amyloid angiopathy in the aetiology and immunotherapy of Alzheimer disease. Alzheimer's. *Res Ther*. 2009;1:6-6. https://doi.org/10.1186/alzrt6
32. Hutmacher M, Hu C, Guenzler-Pukall V, et al. Pharmacokinetic-pharmacodynamic modeling of amyloid-related imaging abnormalities of edema following intravenous administration of bapineuzumab to subjects with mild to moderate Alzheimer's disease. *J. Pharmacokinet. Pharmacodyn.*. 2013;40, Abstract W-040 S015-S149.
33. Gieschke R, Retout S, Frey N, et al. Amyloid related imaging abnormalities (ARIA): time to event modeling to identify new Phase 3 doses and dosing regimens for Gantenerumab. *PAGE*. 2016;25 Abstr 5878.
34. Muralidharan KK, Karumanchi S, Kowalski KG, et al. A time-to-event exposure-response model for amyloid-related imaging abnormalities following administration of aducanumab to subjects with early alzheimer's disease. *J Clin Pharmacol*. 2022;0(0):1-17. https://doi.org/10.1002/jcph.2047
35. Klein G, Delmar P, Rehal S, et al. *Consistently Large Amyloid Reduction in Patients With and Without ARIA-E in the Gantenerumab SCarlet RoAD and Marguerite RoAD OLE Studies*. ADPD; 2019.
36. Liu E, Wang D, Sperling R, et al. Biomarker pattern of ARIA-E participants in phase 3 randomized clinical trials with bapineuzumab. *Neurology*. 2018;90:e877-e886. https://doi.org/10.1212/wnl.0000000000005060

SUPPORTING INFORMATION

Additional supporting information can be found online in the Supporting Information section at the end of this article.

How to cite this article: Aldea R, Grimm HP, Gieschke R, et al. In silico exploration of amyloid-related imaging abnormalities in the gantenerumab open-label extension trials using a semi-mechanistic model. *Alzheimer's Dement*. 2022;8:e12306. https://doi.org/10.1002/trc2.12306